Taylor & Francis
Taylor & Francis Group

Automatika

Journal for Control, Measurement, Electronics, Computing and Communications

ISSN: (Print) (Online) Journal homepage: https://www.tandfonline.com/loi/taut20

Predictive extended state observer-based repetitive controller for uncertain systems with input delay

V. Artheec Kumar, Zhenwei Cao, Zhihong Man, Raymond Chuei & Don Bombuwela

To cite this article: V. Artheec Kumar, Zhenwei Cao, Zhihong Man, Raymond Chuei & Don Bombuwela (2022) Predictive extended state observer-based repetitive controller for uncertain systems with input delay, Automatika, 63:1, 122-131, DOI: 10.1080/00051144.2021.2011686

To link to this article: https://doi.org/10.1080/00051144.2021.2011686

Published online: 09 Dec 2021.

AUTOMATIKA
2022, VOL. 63, NO. 1, 122–131
https://doi.org/10.1080/00051144.2021.2011686

Predictive extended state observer-based repetitive controller for uncertain systems with input delay

V. Artheec Kumar, Zhenwei Cao, Zhihong Man, Raymond Chuei and Don Bombuwela

Faculty of Science, Engineering and Technology, Swinburne University of Technology, Melbourne, Australia

ABSTRACT

This article presents a predictive extended state observer-based repetitive controller (PESO-RC) to simultaneously track and reject periodic signals on systems with long input delay and parameter uncertainties. First, a novel extended state observer (ESO) is proposed to tackle periodic signals on processes with input delay. Then a simple low pass filter is incorporated and tuned to improve robustness against modelling errors. Moreover, the modified repetitive controller (MRC) is integrated to enhance the performance when compensating periodic signals without affecting the overall system's stability. Stability criteria and robust stability analysis under modelling errors are studied to develop tuning guidelines. Furthermore, validation of the proposed controller and comparison studies are simulated in MATLAB and tested on a brushless DC servo motor which highlight the superior performance of PESO-RC.

ARTICLE HISTORY
Received 29 December 2020
Accepted 12 November 2021

KEYWORDS
Extended state observer; repetitive control; time delay systems; Smith predictor; robust control

1. Introduction

Input delays, parameter uncertainties and external disturbances are unavoidable aspects of most real-world systems, leading to performance degradation or even instability of the overall system. Hence, careful consideration of such phenomenon in systems is essential when designing a controller.

Input delay can be due to various reasons such as transmission, propagation of material or information and computation [1]. Delays are present in many real-world structures such as network control, process control, vision control, etc. The Smith Predictor (SP) technique [2] is one of the original works for input delay compensation. Assuming accurate modelling, SP allows the closed-loop characteristic equation to be delay-free. However, it cannot provide satisfactory performance when external disturbances or model errors are present. Further, the SP can only be utilised for open-loop stable systems with constant delay. Hence, several unified and robust SP methodologies were proposed to accommodate all types of systems with parameter uncertainties and time-varying delays [3–5]. The above controllers can effectively reject step disturbances. However, they have significant errors when rejecting periodic disturbances. Hence, the idea was further improved in [6,7] to allow the rejection of periodic disturbances. However, these controllers are highly reliant on the inverse plant model and are not intended to track and reject periodic signals simultaneously.

As previously mentioned, disturbance and uncertainties exist in all systems and processes, which leads to modelling errors. Hence, proposals of several observer or estimator based controllers to deal with external disturbances and unknown plant dynamics are prominent in academia. Unknown input observers [8], Interval observers [9,10], Extended state observers are popular research areas amongst them. Exceptionally, ESO based controllers can provide significant performance with minimal model information. This allows the observer technique easy to implement, making it an attractive concept for many scholars. Han et al. introduced ESO with nonlinear gains [11], while a simple linear ESO was derived in [12]. In recent years to deal with uncertain time-delay systems, researchers have proposed various ESO based algorithms [13–15]. Remarkably, Smith Predictor based ESO (SPESO) was utilised by Zheng et al. [13] to compensate systems with dominant input delays. Nevertheless, with all techniques mentioned above, a significant error at steady-state is unavoidable when compensating for periodic signals. Authors are not aware of much progress in the field of ESO based controllers to deal with periodic signals on processes with considerable input delay. Although, proposals stated above benefited from the intrinsic capability of ESO to deal with plant parameter uncertainty, robustness against delay uncertainties was not achieved.

The compensation of periodic signals is equally vital and has various applications [16,17] in control

CONTACT V. Artheec Kumar avickneswaran@swin.edu.au

This article has been corrected with minor changes. These changes do not impact the academic content of the article.

engineering. Repetitive Control (RC) is a technique explicitly proposed to tackle the requirement mentioned above [18] and was stemmed from the concept of the Internal Model Principle (IMP) [19]. However, RC was initially proposed for systems with no inherent input delay. Hence, researchers have proposed RC structures to compensate systems with input delay [20–22] while dealing with periodic signals. Notably, Na et al. presented a repetitive controller for systems with input delay in [22]. This idea benefited from including an additional delay such that the overall input delay is equal to the smallest positive integer multiple of the period to be tracked and used a Disturbance Observer to deal with disturbance rejection. However, the algorithms proposed above resulted in poor performance when applied to uncertain systems. Further, despite the proposal of ESO based RC [23] to deal with signals of periodic nature on uncertain systems, direct application of these controllers on systems with significant input delay resulted in instability of the overall system.

This paper proposes a novel algorithm to simultaneously track and reject periodic signals on uncertain systems with substantial input delay. Motivated to utilise ESO's robust nature, a novel ESO based controller is proposed to tackle periodic signals on systems with input delay using SP methodology. To improve robustness against both plant parameter and delay uncertainties, a simple low pass filter (LPF) is suggested with tuning guidelines. PESO-RC is restricted for open-loop stable systems. Utilising the filter proposed in [14], the SP could have been modified to control all types of processes. However, a trivial low pass filter is used to target only the robustness of the controller while maintaining the algorithm's simplicity. Then MRC is effectively integrated to enhance the performance when tracking or rejecting periodic signals without affecting the overall system's stability.

Furthermore, PESO-RC is easy to tune with only three tuning parameters. ESO design needs tuning of two parameters to place the controller and observer poles appropriately, while the last parameter will adjust the LPF to improve robustness. The preliminary work of this algorithm was reported in [24], where the controller was developed for first-order plants with input delay to deal with periodic signals.

The remainder of this article is organised as follows. PESO-RC design is demonstrated in section 2. The stability condition of this controller is studied in section 3, and robustness stability analysis is carried out in section 4. Section 5 provides rigorous simulative and experimental comparisons and validations. Finally, the conclusion is stated in section 6.

2. Design of PESO-RC

2.1. Design of standard ESO

The implementation of ESO is studied on a second-order plant model shown in (1), with a gain of K, a damping factor of D, a time constant of T and no delays present in the system.

$$P(s) = \frac{Y_p(s)}{U(s)} = \frac{K}{T^2s^2 + 2DTs + 1} \tag{1}$$

The above equation can simplify and be written in the time domain as:

$$\ddot{y}_p(t) = f(t) + b_0u(t) \tag{2}$$

The sum of internal parameter uncertainties and external disturbances is denoted as $f(t)$, defining the generalised disturbance. Compared to the traditional State Observer, in addition to the estimation of states, ESO delivers an estimate for $f(t)$, which can later be compensated through disturbance rejection. Equation (2) can be represented in state-space as below,

$$\begin{aligned}\begin{bmatrix}\dot{x}_{p1}(t)\\ \dot{x}_{p2}(t)\\ \dot{x}_{p3}(t)\end{bmatrix} &= \begin{bmatrix}0 & 1 & 0\\ 0 & 0 & 1\\ 0 & 0 & 0\end{bmatrix}\begin{bmatrix}x_{p1}(t)\\ x_{p2}(t)\\ x_{p3}(t)\end{bmatrix}\\ &\quad + \begin{bmatrix}0\\ b_0\\ 0\end{bmatrix}u(t) + \begin{bmatrix}0\\ 0\\ 1\end{bmatrix}\dot{f}(t)\\ y_p(t) &= \begin{bmatrix}1 & 0 & 0\end{bmatrix}\begin{bmatrix}x_{p1}(t)\\ x_{p2}(t)\\ x_{p3}(t)\end{bmatrix}\end{aligned} \tag{3}$$

where,

$$\begin{bmatrix}x_{p1}(t)\\ x_{p2}(t)\\ x_{p3}(t)\end{bmatrix} = \begin{bmatrix}y_p(t)\\ \dot{y}_p(t)\\ f(t)\end{bmatrix} \tag{4}$$

Equation (3) can be simplified as

$$\begin{aligned}\dot{x}_p(t) &= A_px_p(t) + B_pu(t) + E_d\dot{f}(t)\\ y_p(t) &= C_px_p(t)\end{aligned} \tag{5}$$

An ESO represented by the state space equation (6) is necessary to estimate the states of $x_p(t)$.

$$\begin{aligned}\dot{\hat{x}}_p(t) &= A_p\hat{x}_p(t) + B_pu(t) + L(y_p(t) - \hat{y}_p(t))\\ \hat{y}_p(t) &= C_p\hat{x}_p(t)\end{aligned} \tag{6}$$

where the observer gains are represented as

$$\boldsymbol{L} = [l_1 l_2 l_3]^T \tag{7}$$

Assuming precise estimation from ESO, $u(t)$ can be stated as

$$u(t) = \frac{u_0(t) - \hat{f}(t)}{b_0} = \frac{u_0(t) - \hat{x}_{p3}(t)}{b_0} \tag{8}$$

Upon substituting (8) in (2), the plant can reduce to

$$\ddot{y}_p(t) = \{f(t) - \hat{f}(t)\} + u_0(t) \approx u_0(t) \tag{9}$$

The error between states of the system and the observer is given by

$$x_e(t) = x_p(t) - \hat{x}_p(t) \tag{10}$$

Subtracting (6) from (5), we obtain

$$\dot{x}_e(t) = [A_p - LC_p]x_e(t) + E_d\dot{f}(t) \tag{11}$$

The extended state observer is BIBO stable if $[A_P - LC_P]$ has roots in the left half of the s-plane, and $f(t)$ is Lipschitz. As per the recommendation of [12], all poles of ESO are located in the same position, P_{ESO}. From this, the controller can be equated as (12).

$$u_0(t) = k_1(r(t) - \hat{x}_{p1}(t)) - k_2\hat{x}_{p2}(t) \tag{12}$$

where k_1 and k_2 are the controller gains.

2.2. Design of SP based ESO

Conventional ESO implemented on a system consisting of input delay will result in a deviation of estimations from ESO compared to actual states of the plant. If the dead time is significant, it may even result in an unstable overall system. Now let us study the plant discussed in (1) with substantial delay, $\mathrm{l_p}$ in the input channel.

$$\frac{Y_p(s)}{U(s)} = \frac{K}{T^2s^2 + 2DTs + 1}e^{-sl_p} \tag{13}$$

With the input delay present, there is a timewise misalignment of actual plant output and the output estimated by ESO. The current relationship between the delayed plant output and the ESO output at a steady state is given below.

$$y_p(t + l_p) = \hat{y}_p(t) \tag{14}$$

With ESO having the state space relationship illustrated in (6), it is clear the observer error does not match in time if the delay influenced plant output, $y_p(t)$ is used directly. From (14), it can be noticed that the misalignment can be fixed if $y_p(t)$ is substituted by signal $y_p(t + l_p)$. Methods of prediction can obtain this. From the concept of SP, the predicted output $y_{sp}(t)$ can be created as:

$$y_{sp}(t) = y_p(t) - y_m(t) + y_m(t + l_m) \tag{15}$$

where y_m(t) and l_m are nominal models of $y_p(t)$ and l_p, respectively. With model matching condition assumed, (15) can be written as:

$$y_{sp}(t) = y_p(t + l_p) = C_p x_p(t) \tag{16}$$

As shown above, with the aid of the Smith Predictor, the delay effect on the plant output can be avoided, given that the plant is open-loop stable. This allows both inputs to the ESO to be synchronised in the dimension of time. The modified ESO can now be represented in state-space as below.

$$\begin{aligned}\dot{\hat{x}}_p(t) &= A_p\hat{x}_p(t) + B_p u(t) + L(y_{sp}(t) - \hat{y}_p(t))\\ \hat{y}_p(t) &= C_p\hat{x}_p(t)\end{aligned} \tag{17}$$

The controller assumes accurate modelling. Hence, $y_{sp}(t)$ is free from delay, resulting in (16). However, when there are modelling errors, the above is not valid, leading to the low robustness of the controller. Moreover, the delay element attached to input disturbance $w_1(t)$ is not cancelled by the predictor before entering ESO. Hence, the disturbance estimation will occur with a delay of l_p. This does not affect steady-state performance when rejecting step signals but causes an unavoidable error when rejecting periodic signals at steady-state. Moreover, the plant's output is delayed by l_p, making accurate tracking of periodic signals in time not possible.

2.3. Design of the proposed controller

To deal with periodic signals, a novel predictive ESO based RC technique is proposed. The general design of PESO-RC is illustrated in Figure 1. The input delay of the system is further delayed by an additional delay term τ, such that the overall delay of the system is equal to nT_P. The period of the signal to be tracked or rejected would be given as T_P, and n is chosen as the minimum positive integer required to make τ greater than zero. The SP is devised to deal with the delay of nT_p compared to l_m.

The disturbance entering ESO is delayed now by nT_p. Due to the periodic nature of the signals, the actual input disturbance is synchronised in time with the estimated disturbance, allowing good rejection. Besides, the output is now delayed by nT_p, allowing perfect tracking in time.

The effects of modelling errors on Y_{sp} (s) are exhibited on higher frequencies [25], resulting in potential instability of the overall system. Hence, a LPF $q_2(s)$ is incorporated into SP to reduce the impact of the model mismatch at high frequencies and improve robustness. The transfer function of predicted output $Y_{sp}(s)$ can be now constructed as:

$$Y_{sp}(s) = q_2(s)\{Y_p(s) - Y_m(s)\} + Y_m(s)e^{snTp} \tag{18}$$

Finally, to further improve the controller's performance when compensating periodic signals, a plug-in MRC is included in the feed-forward path. The tracking error of the system $e(t)$ can be written as

$$e(t) = r(t) - \hat{x}_{p1}(t) \tag{19}$$

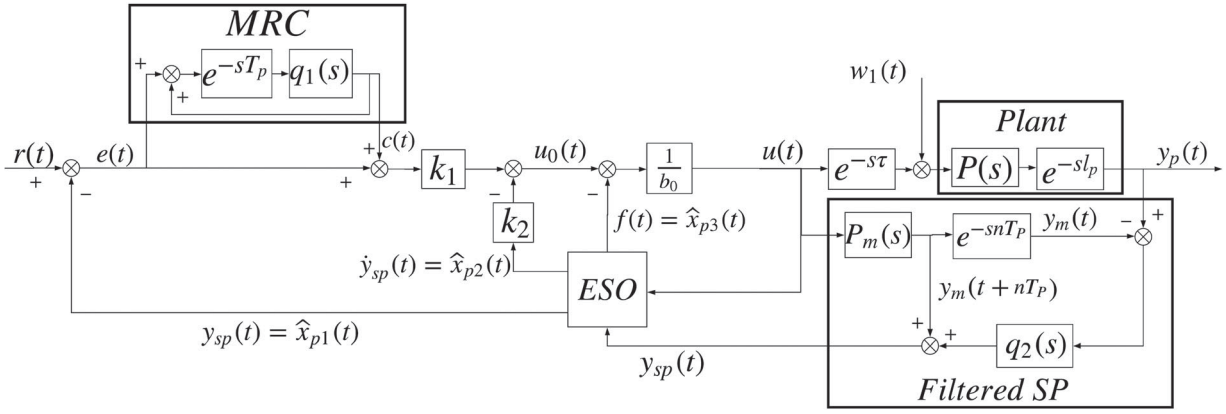

Figure 1. Block diagram of PESO-RC.

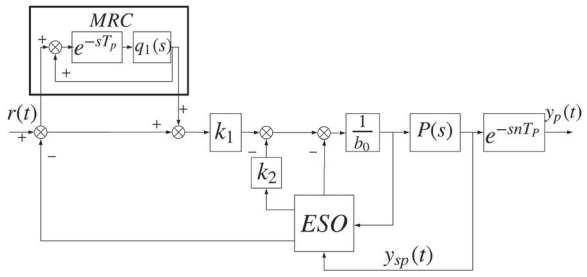

Figure 2. ESO based RC under model matching condition.

MRC can be illustrated with the following transfer function.

$$G_{rc}(s) = \frac{C(s)}{E(s)} = \frac{q_1(s)e^{-sTp}}{1 - q_1(s)e^{-sTp}} \tag{20}$$

If the ESO is precisely designed, (8) can represent the equation of controller, and the control law of PESO-RC can be given as

$$u_0(t) = k_1[r(t) + c(t) - \hat{x}_{p1}(t)] - k_2\hat{x}_{p2}(t) \tag{21}$$

3. Stability analysis

Let us assume the plant is open-loop stable, with the model matching condition. An equivalent block diagram of the system is depicted in Figure 2.

Since the model matching condition is assumed, there is no limitation on the cut-off frequency of $q_2(s)$. Hence it can be taken as unit gain. From the above figure, it can be noticed that the system is similar to ESO based ADRC with a plug-in RC in the feedforward path proposed in [23]. However, the output is delayed by nT_p.

Now let us consider the closed-loop system without RC by making $c(t)$ equal to zero. This is the same as the design of ESO based ADRC explained in section 2.1, but the output is delayed as mentioned above. However, the delay is outside the feedback loop, and only the predicted output is fed to the ESO. This removes the limitation on stability exerted by the delay. The plant and the ESO state-space equation will be as follows

$$\begin{aligned} \dot{x}_p(t) &= A_p x_p(t) + B_p u(t) + E_d \dot{f}(t) \\ y_p(t) &= C_p x_p(t) e^{-sn(Tp)} \end{aligned} \tag{22}$$

$$\begin{aligned} \dot{\hat{x}}_p(t) &= A_p \hat{x}_p(t) + B_p u(t) + L(y_{sp}(t) - \hat{y}_p(t)) \\ \hat{y}_p(t) &= C_p \hat{x}_p(t) \end{aligned} \tag{23}$$

Considering the nominal plant is completely state controllable and observable, then by substituting (21) in (8) with $c(t)$ equal to zero, we obtain,

$$u(t) = \frac{1}{b_0}\{k_1(r(t) - \hat{x}_{p1}(t)) - k_2\hat{x}_{p2}(t) - \hat{x}_{p3}(t)\} \tag{24}$$

Equation (24) can be rewritten as

$$u(t) = \frac{k_1}{b_0} r(t) - \frac{\boldsymbol{K}}{b_0}\hat{x}_p(t) \tag{25}$$

where

$$\mathbf{K} = [\mathbf{k}_1 \mathbf{k}_2 1] \tag{26}$$

By substituting (25) in (22), we obtain

$$\dot{x}_p(t) = A_p x_p(t) + B_p\left(\frac{k_1}{b_0} r(t) - \frac{\boldsymbol{K}}{b_0}\hat{x}_p(t)\right) + E_d \dot{f}(t) \tag{27}$$

Rearranging (27)

$$\begin{aligned} \dot{x}_p(t) = (A_p - B_p\boldsymbol{K}_0)x_p(t) + B_p\boldsymbol{K}_0(x_p(t) - \hat{x}_p(t)) \\ + B_p F_r r(t) + E_d \dot{f}(t) \end{aligned} \tag{28}$$

where,

$$\begin{bmatrix} \boldsymbol{K}_0 \\ F_r \end{bmatrix} = \frac{1}{b_0}\begin{bmatrix} \boldsymbol{K} \\ k_1 \end{bmatrix} \tag{29}$$

Incorporating error vector from (10) and substituting in to (28) gets

$$\begin{aligned} \dot{x}_p(t) = (A_p - B_p\boldsymbol{K}_0)x_p(t) + B_p\boldsymbol{K}_0 x_e(t) \\ + B_p F_r r(t) + E_d \dot{f}(t) \end{aligned} \tag{30}$$

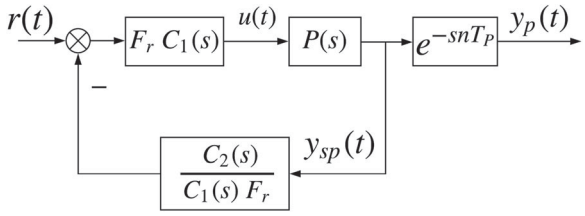

Figure 3. Control system with ESO.

From (28) and (11), state-space representation of system and error can be given as

$$\begin{bmatrix}\dot{x}_p(t)\\ \dot{x}_e(t)\end{bmatrix} = \begin{bmatrix}A_p - B_p\boldsymbol{K}_0 & B_p\boldsymbol{K}_0\\ 0 & A_p - \boldsymbol{L}C_p\end{bmatrix}\begin{bmatrix}x_p(t)\\ x_e(t)\end{bmatrix} + \begin{bmatrix}B_pF_r & E_d\\ 0E_d & \end{bmatrix}\begin{bmatrix}r(t)\\ \dot{f}(t)\end{bmatrix} \tag{31}$$

The characteristic equation of (31) is given below.

$$|sI - A_p + B_p\boldsymbol{K}_0| = 0 \text{ and } |sI - A_p + \boldsymbol{L}C_p| = 0 \tag{32}$$

From (32), it can be noted that the pole placement for controller and observer can be designed independently of each other to ensure the stability of the overall system. Besides, the system input needs to be bounded. Hence, $r(t)$ and derivative of $f(t)$ need to be bounded signals.

Taking Laplace transformation of (23) and (25) will result in the following equation,

$$s\hat{X}_p(s) = A_p\hat{X}_p(s) + B_pU(s) + \boldsymbol{L}(Y_{sp}(s) - \hat{Y}_p(s)) \tag{33}$$

$$U(s) = F_rR(s) - \mathbf{K}_0\hat{X}_p(s) \tag{34}$$

Given $U(s) = Y_{SP}(s)/P(s)$, we get

$$Y_{sp}(s) = \frac{C_1(s)F_rP(s)}{1 + C_2(s)P(s)}R(s) = G_{\mathrm{CL}}(s)R(s) \tag{35}$$

where

$$C_1(s) = 1 - \boldsymbol{K}_0(sI - A_p + B_p\boldsymbol{K}_0 + \boldsymbol{L}C_p)^{-1}B_p \tag{36}$$

$$C_2(s) = \boldsymbol{K}_0(sI - A_p + B_p\boldsymbol{K}_0 + \boldsymbol{L}C_p)^{-1}\boldsymbol{L} \tag{37}$$

Figure 3 shows the control system based on ESO, and its closed-loop transfer function is G_{CL}.

Figure 4 depicts the equivalent block diagram of ESO based plug-in RC illustrated in Figure 2.

From Figure 4, the system's stability is ensured, given that the following are valid [18].

Condition 1 : $\mathrm{G_{CL}(s)}$ obtained in (35) is stable

$$\textbf{Condition } 2: \quad \frac{q_1(s)}{1 + P(s)\ C_2(s)}_{\infty} < 1$$

Remark 3.1: From (32), G_{CL} is stable if the $eig(A_p - B_p\boldsymbol{K_0})$ and $eig(A_p - LC_p)$ poles in the left half side of

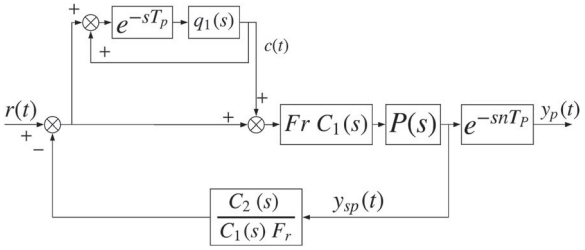

Figure 4. ESO based RC system.

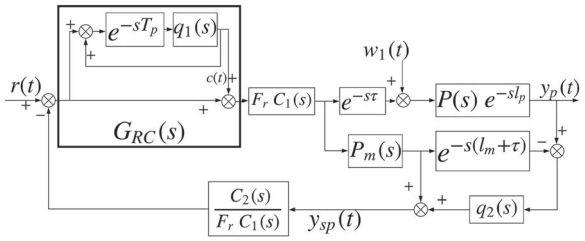

Figure 5. Control of PESO-RC under parameter uncertainty.

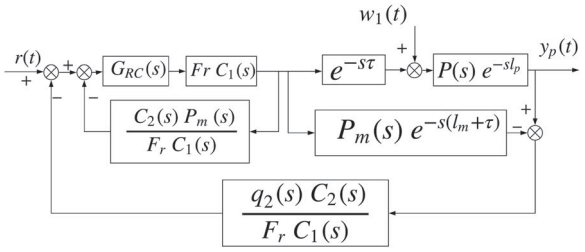

Figure 6. IMC interpretation of PESO-RC control system.

the Imaginary axis in the s-plane, satisfying **Condition 1**. This can be achieved when the ESO based controller is designed. Provided **Condition 1** is valid, and **Condition 2** is achieved with the appropriate tuning of the low pass filter $q_1(s)$, from the Small gain theorem overall system is stable.

4. Robustness stability with parameter uncertainties

In real-world applications, parameter uncertainties are unavoidable. In that case, the stability analysis derived in Section 3 is not sufficient as it assumes perfect model matching. From (36), (37) and the assumption of uncertain plant parameters, Figure 1 can be redrawn as Figure 5.

To study the robustness, we will use the Internal Model Control (IMC) interpretation of the PESO-RC based control system. IMC interpretation of the control system is derived in the block diagram illustrated in Figure 6.

where,

$$G_{RC}(s) = \frac{1}{1 - q_1(s)e^{-sT_P}} \tag{38}$$

We will further simplify to obtain the control system in 2DOF-IMC structure, as illustrated in Figure 7,

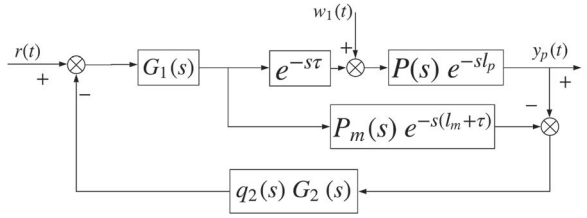

Figure 7. 2DOF-IMC structure of PESO-RC control system.

where,

$$G_1(s) = \frac{F_r C_1(s) G_{RC}(s)}{1 + P_m(s) C_2(s) G_{RC}(s)} \tag{39}$$

$$G_2(s) = \frac{C_2(s)}{F_r C_1(s)} \tag{40}$$

The characteristic equation of the above system with modelling errors can be given as

$$1 + q_2(s) G_2(s) e^{-s\tau} (P(s) e^{-sl_p} - P_m(s) e^{-sl_m}) G_1 \tag{41}$$

Let $\Delta P(s) = P(s)e^{-sl_p} - P_m(s)e^{-sl_m}$, where ΔP is the addictive uncertainty, and the robust stability for the scheme in Figure 1 is given as

Condition 3

$$|G_2(s)\Delta P(s) G_1(s)| < \frac{1}{|q_2(s)|}|_{s=j\omega} \forall\, \omega > 0 \tag{42}$$

Remark 3.2: The overall system is robustly stable provided both **Condition 1** and **Condition 2** are met in addition to achieving **Condition 3** by appropriate tuning of the low pass filter $q_2(s)$. The above is derived from the well-known Small gain theorem.

5. Simulative and experimental results

Design procedure coupled with simulation and experimental analysis of PESO-RC is presented in this section. Furthermore, this section discusses the comparison of tracking, disturbance rejection and validation of robustness of the proposed controller.

The design procedure for PESO-RC is given below

(1) From the system model, choose $b_0 = K/T^2$ and set τ such that $\tau + l_m = nT_P$.
(2) Choose P_{CL} using the equation below such that a 2% settling time can be obtained.

$$P_{\text{CL}} = -\frac{6}{T_{\text{settle}}} \tag{43}$$

where P_{CL} denotes the desired position of the closed-loop pole, and the anticipated setting time is indicated by T_{settle}.
(3) The state feedback gains can be determined by solving the following quadratic equation.

$$(s - P_{\text{CL}})^2 = s^2 - 2P_{\text{CL}}s + P_{\text{CL}}^2 \tag{44}$$

From solving above equation, $k_1 = (P_{\text{CL}})^2$ and $k_2 = -2P_{\text{CL}}$

(4) To obtain accurate results, the poles of the ESO must be positioned further to the left of P_{CL}. Hence, choose observer poles as P_{ESO} such that they are 3–5 times greater than P_{CL}. As per bandwidth parameterisation [12], place all observer poles in one location. The observer gains can be obtained by solving the following third order equation

$$(s - P_{ESO})^3 = s^3 - 3P_{ESO}s^2 + 3P_{ESO}^2 s - P_{ESO}^3 \tag{45}$$

From solving above equation, $l_1 = -3P_{ESO}$, $l_2 = 3(P_{ESO})^2$ and $l_3 = -(P_{ESO})^3$

(5) Implement Smith Predictor as illustrated in (18) to synchronise both inputs of the ESO.
(6) With the model matching condition assumed, there is no limitation on the bandwidth of LPF, $q_2(s)$. Design a low pass filter $q_1(s)$ such that **Condition 2** is true. However, if there is a model mismatch, then the cut-off frequency of LPF $q_2(s)$ should be chosen, such that (42) is true. For ease of design, the smallest cut off frequency can be chosen as the cutoff frequency for both $q_1(s)$ and $q_2(s)$.

5.1. Simulated performance without uncertainties

The simulative tracking performance and disturbance rejection are discussed here. Using MATLAB and Simulink, the capability of the proposed controller has been demonstrated. A perfect model matching condition is assumed, and a period of $T_P = 8$ s is selected for reference input or disturbances where $f_P = 1/8$ Hz. PESO-RC is compared against MSP-PI proposed by Zhou et al. [6] and RCDO presented by Na et al. [22].

We consider a model of a second-order plant consisting of an input delay with the transfer function:

$$P_m(s)e^{-sl_m} = \frac{344.42}{s^2 + 37.12s + 344.42} e^{-3s} \tag{46}$$

PESO-RC parameters are designed with $b_0 = 344.42$ and $T_{\text{settle}} = 0.15$ s. The other parameters are obtained by design procedures 3, 4 to design a stable ESO based system to satisfy **Condition 1**. τ is set to 5 s such that $\tau + l_m$ is equal to T_P, which is 8 s. According to procedure 5, the Smith predictor is implemented to ensure synchronisation of the inputs of the ESO. The low pass filter, $q_1(s)$ in PESO-RC, is designed with a cut off frequency of 20 rad/s to provide adequate bandwidth to handle the harmonics of reference and disturbance signals while ensuring **Condition 2** is satisfied. Due to the model matching assumption equation (42) is true when

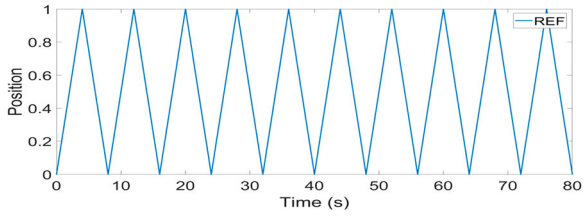

Figure 8. Reference input signal.

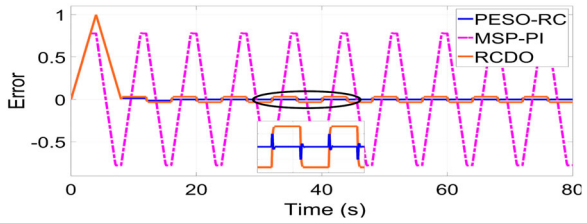

Figure 9. Simulative tracking error.

$q_2(s)$ is unit gain. The cut-off frequency of the LPF in RCDO is tuned to be 20 rad/s to provide similar tuning conditions with an additional delay of 5 s included in the feedforward path. For MSP-PI, the PI controller G_{c1} is set as $0.51 + 9.47/s$ while ξ, N and h are chosen as 0.7, 175 and 5 respectively to achieve G_{c3}.

To compare tracking performance, a reference signal of a triangular wave as shown in Figure 8 with an amplitude of 1 V is introduced with no input disturbance initially. The results illustrated in Figure 9 clearly shows MSP-PI is not capable of precise tracking in time while PESO-RC provides accurate tracking compared to RCDO.

To analyse the disturbance rejection performance, the effect of four periodic disturbances is studied with no requirement to track a reference signal where $r(t) = 0$. The disturbance signals are introduced as input disturbance $w_1(t)$, where,

$$d_1(t) = -\frac{1}{2}\sin(2\pi f_{pr}t) \tag{47}$$

$$d_2(t) = -\frac{1}{2}\sin(2\pi f_{pr}t) - \frac{1}{2}\sin(2\pi(3f_{pr})t) \tag{48}$$

$d_3(t)$: Triangular wave with an amplitude of -0.5V and period of 8s (49)

$d_4(t)$: Sum of traingular singals of period 8s and 4s with amplitude of -0.5V (50)

Figures 10–13 present the comparative results of simulative tracking errors. Though all controllers can reject periodic signals, from the results below, it is evident that the PESO-RC provides superior disturbance rejection of periodic signals.

On the other hand, to show the performance enhancement by RC, we compare the proposed controller with and without plug-in RC, and the results are illustrated in Figure 14. The control requirement is to track the same reference signal shown in Figure 8

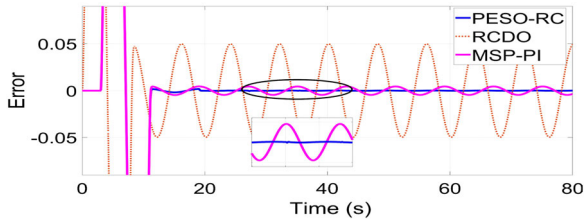

Figure 10. Simulative error with $d_1(t)$.

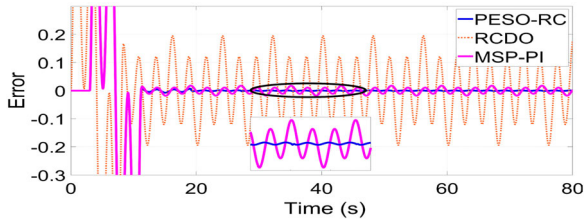

Figure 11. Simulative error with $d_2(t)$.

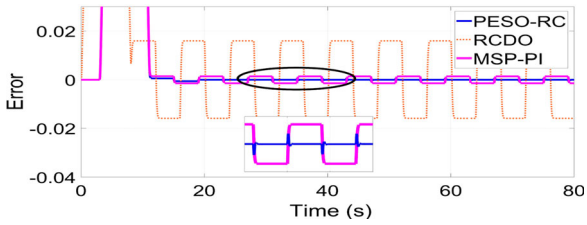

Figure 12. Simulative error with $d_3(t)$.

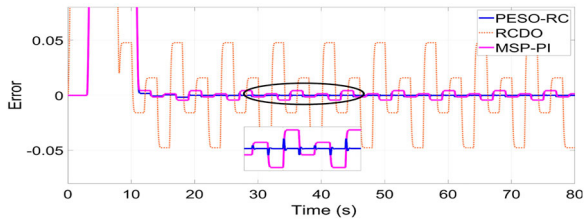

Figure 13. Simulative error with $d_4(t)$.

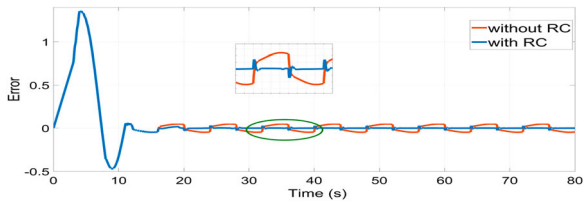

Figure 14. Error of proposed control with and without RC.

while rejecting the input disturbance of $w_1(t)$ described in (47). From the results, it can be determined that the inclusion of RC improves performance considerably (Figure 15).

5.2. Experimental analysis

In order to verify the reliability of the controller further, the proposed controller is applied in a real-world application. A Model 220 Emulator Apparatus from ECP

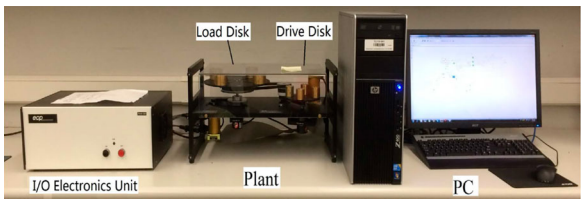

Figure 15. Hardware setup of the experimental system.

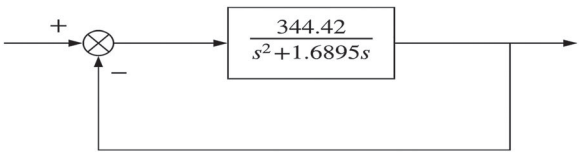

Figure 16. Block diagram of the modified plant.

is chosen as the experimentation system. This consists of an emulator mechanism, actuator and sensors. The hardware also features brushless DC servo motors for load, drive and disturbance generation. The model of the system is not precisely known. We can approximately model it as a second-order plant, and it is given as (51).

$$P_{m\_servo}(s) = \frac{344.42}{s^2 + 1.6895s} \tag{51}$$

To achieve a stable plant, the system is modified, as suggested in Figure 16. The transfer function of the modified plant can be considered as

$$P_m(s) = \frac{344.42}{s^2 + 1.6895s + 344.42} \tag{52}$$

In order to validate the controller for time-delay systems, an input delay of 3 s is simulated and added to the forward path of the control system such that

$$P_m(s)e^{-sl_m} = \frac{344.42}{s^2 + 1.6895s + 344.42}e^{-3s} \tag{53}$$

The PESO-RC is compared against RCDO and SPESO proposed by Zheng et al. [13]. PESO-RC and SPESO parameters are designed with $b_0 = 344.42$ and $T_{\text{settle}} = 0.25$s. Design procedures 3 and 4 are used to derive other parameters for designing a stable control system based on ESO to satisfy **Condition 1**. For PESO-RC, τ again is set to 5s. According to procedure 5, Smith predictors are implemented for PESO-RC and SPESO to ensure synchronisation of the inputs of the extended state observer. The cut-off frequency of the LPF, $q_1(s)$ in PESO-RC is assigned to be 25 rad/s such that **Condition 2** is satisfied. As recommended by step 6 of the design procedure, $q_2(s)$ is also tuned with a cut-off frequency of 25 rad/s to account for the unpredictable dynamics of the experiment system. The low pass filter in RCDO is assigned with a cut-off frequency of 25 rad/s to provide similar tuning conditions with an additional delay of 5 s included in the feedforward path.

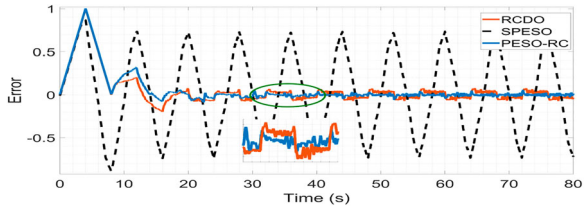

Figure 17. Experimental tracking error with no disturbance.

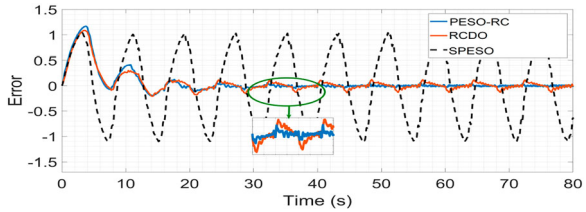

Figure 18. Experimental tracking error with $d_1(t)$.

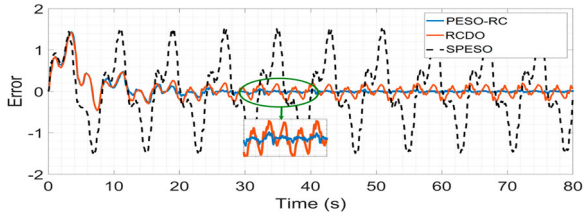

Figure 19. Experimental tracking error with $d_2(t)$.

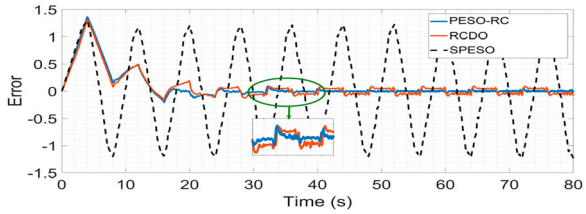

Figure 20. Experimental tracking error with $d_3(t)$.

Table 1. Comparison of experimental RMSE

Disturbance	PESO-RC	RCDO
$w_1(t) = 0$	0.0147	0.0390
$w_1(t) = d_1(t)$	0.0142	0.0524
$w_1(t) = d_2(t)$	0.0185	0.1131
$w_1(t) = d_3(t)$	0.0149	0.0532
$w_1(t) = d_4(t)$	0.0160	0.0636

The control objective is to simultaneously track the periodic signal shown in Figure 8 while rejecting the disturbances used in the simulative comparison.

Figures 17–21 illustrate the experimental tracking errors of the control system with the corresponding input disturbances. RMSE at steady state is compared in Table 1. The error of controllers after the fourth period is used to find steady-state RMSE. Similar to the results obtained from the simulation analysis, PESO-RC has better capacity than RCDO when dealing with periodic signals, while SPESO does not provide satisfactory performance.

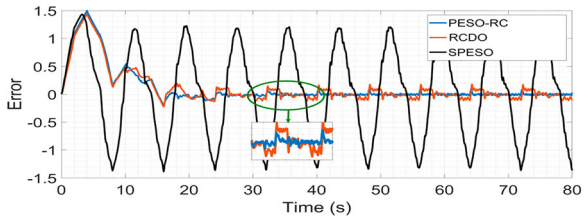

Figure 21. Experimental tracking error with $d_4(t)$.

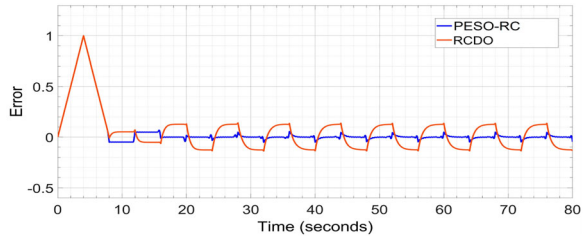

Figure 22. Tracking error under parameter uncertainties.

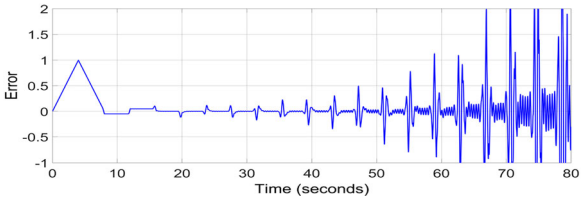

Figure 23. Tracking error of PESO-RC when $q_2(s) = 1$.

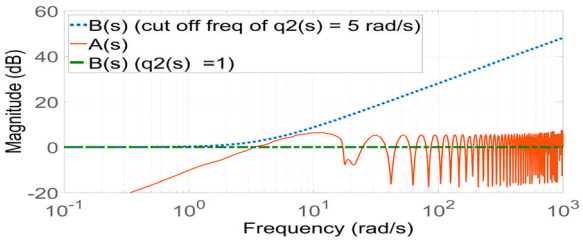

Figure 24. Robustness criterion against frequency.

5.3. *Simulative robustness analysis*

The robustness against the modelling error of the proposed controller is validated in this section. Though the plant is modelled by (53), let us consider the actual plant's transfer function as

$$P(s)e^{-sl_p} = \frac{300}{s^2 + s + 300}e^{-3.3s} \tag{54}$$

The response is studied by allowing the system to track a reference signal, depicted in Figure 8. The performance of the proposed controller is compared with RCDO.

Accounting for uncertainty and as per design procedure 6, for PESO-RC, both Low pass filters $q_1(s)$ and $q_2(s)$ are tuned to have cut-off frequencies at 5 rad/s, such that **Condition 3** is satisfied. To provide similar tuning conditions to RCDO, the cut-off frequency of the low pass filter is reduced to 5 rad/s. The tracking error of both controllers is illustrated in Figure 22. It is evident that the proposed controller is robust against modelling errors while performing better compared to RCDO.

To show the importance of $q_2(s)$ on robustness, low pass filter $q_2(s)$ is replaced with unit gain while no change is made to $q_1(s)$. The results are shown in Figure 23. It can be noted that the tracking error of the proposed controller designed without consideration for uncertainties has diverged despite the reduction of the cut-off frequency in $q_1(s)$.

Given,

$$A(s) = |G_2(s)\Delta P(s)G_1(s)| \tag{55}$$

$$B(s) = \left|\frac{1}{q_2(s)}\right| \tag{56}$$

Figure 24 plots Equation (42) against frequency to verify robustness criterion. This validates the results illustrated in Figure 22 (blue line), where **Condition 3** is met compared to Figure 23 (green line) results from failing to meet the robustness condition. Moreover, from Figure 24, it can be established that with the appropriate tuning of the low pass filter $q_2(s)$, the magnitude of $B(s)$ can be increased at higher frequencies to satisfy **Condition 3** when parameter uncertainties are present in the system.

6. Conclusion

This article recommends a novel controller, PESO-RC, for concurrent tracking and rejecting periodic signals on uncertain systems with significant input delay, proven in simulation and experimental studies. The stability and robustness of the system with the proposed controller are analysed mathematically. From the comparison study, PESO-RC is ideal for compensating periodic signals when accurate performance is required. As future work, other robust observer based control techniques [26,27] will be studied to compensate multibody systems with time delays and aperiodic disturbances.

Disclosure statement

No potential conflict of interest was reported by the author(s).

Funding

This work was supported by the Australian Research Council [grant number DP190101557].

References

[1] Richard JP. Time-delay systems: an overview of some recent advances and open problems. Automatica. October 2003;39:1667–1694.
[2] Smith OJM. Closer control of loops with dead time. Chem Eng Prog. 1957;53:217–219.

[3] Morato MM, Normey-Rico JE. A novel unified method for time-varying dead-time compensation. ISA Trans. August 2020;108:78–95.
[4] Silva LRD, Flesch RCC, Normey-Rico JE. Controlling industrial dead-time systems: when to use a PID or an advanced controller. ISA Trans. April 2020;99:339–350.
[5] Normey-Rico JE, Guzmán JL. Unified PID tuning approach for stable, integrative and unstable dead-time processes. IFAC Proc Vol. 2012;45:35–40.
[6] Zhou HQ, Wang QG, Min L. Modified Smith predictor design for periodic disturbance rejection. ISA Trans. October 2007;46:493–503.
[7] Karanam KC, Sivalingam S, Ambati SR. Modified Smith predictor design for unstable processes with step and periodic disturbances. Proc Inst Mech Eng. March 2013;227:146–160.
[8] Oliveira MS, Pereira RL. On unknown input observers designs for discrete-time LPV systems with bounded rates of parameter variation. Eur J Contr. March 2021;58:183–195.
[9] Khan A, Xie W, Zhang L. Interval state estimation for linear time-varying (LTV) discrete-time systems subject to component faults and uncertainties. Arch Contr Sci. June 2019;29:289–305.
[10] Khan A, Xie W, Zhang B, et al. A survey of interval observers design methods and implementation for uncertain systems. J Frankl Inst. June 2021;358:3077–3126.
[11] Han J. A class of extended state observers for uncertain systems. Contr Decis. 1995;10:85–88.
[12] Gao Z. Scaling and bandwidth-parameterization based controller tuning. Proc. Am. Control Conf., Denver, USA; November 2003. p. 4989–4996.
[13] Zheng Q, Gao Z. Predictive active disturbance rejection control for processes with time delay. ISA Trans. July 2014;53:873–881.
[14] Liu T, Hao S, Li D, et al. Predictor-based disturbance rejection control for sampled systems with input delay. IEEE Trans Contr Syst Technol. March 2019;27:772–780.
[15] Zhang D, Yao X, Wu Q, et al. ADRC based control for a class of input time delay systems. J Syst Eng Electr. December 2017;28:1210–1220.
[16] Doh TY, Ryoo JR, Chung MJ. Design of a repetitive controller: an application to the track-following servo system of optical disk drives. IEE Proc Contr Theory Appl. March 2006;153:323–330.
[17] Grino R, Cardoner R, Costa-Castello R, et al. Digital repetitive control of a three-phase four-wire shunt active filter. IEEE Trans Ind Electr. 2007;54:1495–1503.
[18] Hara S, Yamamoto Y, Omata T, et al. Repetitive control system: a new type servo system for periodic exogenous signals. IEEE Trans Autom Contr. July 1988;37:659–668.
[19] Francis BA, Wonham WM. The internal model principle of control theory. Automatica. September 1976;12:457–465.
[20] Watanabe K, Yamada K. Repetitive control of time-delay systems. 29th IEEE Conf. Decision and Control, Honolulu, USA; 1990. p. 1685–1690.
[21] Tan KK, Zhao S, Huang S, et al. A new repetitive control for LTI systems with input delay. J Proc Contr. April 2009;19:711–716.
[22] Na J, Grino R, Costa-Castello R, et al. Repetitive controller for time-delay systems based on disturbance observer. IET Contr Theory Appl. November 2010;4:2391–2404.
[23] Sayem AHM, Cao Z, Man Z. Model-free ESO-based repetitive control for rejecting periodic and aperiodic disturbances. IEEE Trans Ind Electr. April 2017;64:3433–3441.
[24] Kumar VA, Bombuwela D, Cao Z, et al. Enhanced Smith predictor based active disturbance rejection control for tracking and rejecting periodic signals on time delay systems. 2018 Australian & New Zealand Control Conference, Melbourne; 2018. p. 183–187.
[25] Santacesaria C, Scattolini R. Easy tuning of smith predictor in presence of delay uncertainty. Automatica. November 1993;29:1595–1597.
[26] Khan A, Bai W, Zhang B, et al. Interval state estimator design for linear parameter varying (LPV) systems. IEEE Trans Circ Syst II Express Briefs. Aug 2021;68:2865–2869.
[27] Khan A, Xie W, Liu L. Set-membership interval state estimator design using observability matrix for discrete-time switched linear systems. IEEE Sens J. June 2020;20:6121–6129.